Green Vertical-Cavity Surface-Emitting Lasers Based on Combination of Blue-Emitting Quantum Wells and Cavity-Enhanced Recombination

Rongbin Xu, Yang Mei, Huan Xu, Lei-Ying Ying, Zhiwei Zheng, Hao Long, Dan Zhang, Baoping Zhang, and Jianping Liu

***Abstract*—We fabricated green vertical-cavity surface-emitting lasers by employing $In_xGa_{1-x}N$/GaN quantum wells (QWs) active layers. The In fraction of the QW is 0.18 and the electroluminescence emission peak is around 445 nm, dominantly in the blue. With such QWs embedded in a microcavity, however, lasing was achieved at the emission edge (~493 nm), approaching to the green region. Such phenomenon is attributed to the cavity-enhanced recombination, where the cavity effect and photon–electron interactions or the gain enhancement factor play important roles.**

***Index Terms*—Quantum well (QW) devices, semiconductor lasers, vertical-cavity surface-emitting lasers (VCSELs).**

I. Introduction

TO REALIZE full-color mobile projectors, it is essential to have laser light sources in the three primary RGB colors. The development of a high-performance green laser is one of the most critical issues. Presently, green lasers based on double-frequency technologies are practically used [1], [2]. However, they are big, inefficient, and costly. Thus, semiconductor lasers have attracted significant attention in recent years owing to their small size and low cost [3]. The 2-D InGaN quantum wells (QWs) have been widely used for the active regions of semiconductor lasers that emit in the blue and green regions [4]–[6]. However, it is difficult to achieve InGaN/GaN QWs with both a high indium content and a high material quality compared with low-In-content QWs [7]. In-rich InGaN/GaN QWs are usually accompanied with high density of defects and a large polarization field [8], [9]. The defects result in nonradiative recombination and the large polarization field causes the quantum confinement Stark effect (QCSE) which spatially separates the hole and electron wavefunctions. These issues will decrease the internal quantum efficiency in the green region, resulting in the so-called "green gap" [10].

Vertical-cavity surface-emitting lasers (VCSELs) with planar microcavity structures offer several distinct advantages, including low-divergent output beams, high-speed modulation, and circular beam profiles. They are also easy to fabricate into 2-D arrays [11]. VCSELs are attracting growing attention as demonstrated by the fact that apart from academic researchers [12]–[22], they have been reported also by industrial researchers [23]–[28]. Compared with conventional edge-emitting semiconductor lasers, VCSELs have a much smaller volume and can be classified as microcavity light emitters. In 2011, Nichia first realized a current-injected green GaN-based VCSEL with five pairs of InGaN/GaN QWs as its active region [25]. However, only pulsed operation could be realized and the wavelength was 503 nm. The authors attributed this to the severe QCSE in the high-In-content QWs. Recently, we demonstrated high-performance VCSELs emitting at wavelengths covering most of the "green gap" by using InGaN quantum dot (QD) active regions [20], [21]. The wavelength was extended to 565.7 nm. Moreover, due to the broad spontaneous emission (SE) band, we obtained different lasing wavelengths by tuning the cavity length [21]. However, the growth of QDs is complex and difficult. The output power of the devices is still low (~10 μW).

When the light-emitting medium is placed inside a small resonant cavity, the SE rate at cavity modes will be boosted, which is known as the optical cavity effect. In a cavity, the optical density at the cavity mode is strongly enhanced. Owing to the cavity effect, ON-resonance optical transitions have a much shorter lifetime compared with SEs without a cavity. In the case of a silicon-vacancy center in diamond embedded within a monolithic optical cavity, tenfold lifetime reduction and 42-fold enhancement in emission intensity were observed when the cavity is tuned into resonance with the optical transition of the vacancy [29]. This likewise has

Manuscript received August 9, 2018; accepted August 16, 2018. Date of publication September 3, 2018; date of current version September 20, 2018. This work was supported in part by the National Key Research and Development Program of China under Grant 2016YFB0400803, in part by the National Natural Science Foundation of China under Grant 11474235 and Grant U1505253, and in part by the Science Challenge Project under Grant TZ2016003. The review of this paper was arranged by Editor J. Huang. *(Corresponding authors: Baoping Zhang; Jianping Liu)*

R. Xu, Y. Mei, H. Xu, L.-Y. Ying, Z. Zheng, H. Long, D. Zhang, and B. Zhang are with the Optoelectronics Engineering Research Center, Department of Electronic Engineering, Xiamen University, Xiamen 361005, China (e-mail: bzhang@xmu.edu.cn).

J. Liu is with the Suzhou Institute of Nano-Tech and Nano-Bionics, Chinese Academy of Sciences, Suzhou 215123, China (e-mail: jpliu2010@sinano.ac.cn).

Color versions of one or more of the figures in this paper are available online at http://ieeexplore.ieee.org.

Digital Object Identifier 10.1109/TED.2018.2866406

been demonstrated in GaAs and InGaN QWs [30], [31]. In InGaN/GaN QWs, the emission lifetime may become nearly 10× shorter with a cavity [31].

In this paper, we fabricated green GaN-based VCSELs by combining normally blue-emitting InGaN/GaN QWs with a microcavity. Due to the cavity effect, there are a few resonant modes in the blue (peak at ∼440 nm) and nearly green (peak at ∼493 nm). At lower currents, the blue modes are dominant while with increasing currents, the green modes grow rapidly and finally, reach lasing. The lasing characteristic also benefits from the good coupling between electrons and photons at resonant modes.

II. Materials and Fabrication

The epitaxial structure was grown on a c-plane (0001) sapphire substrate via metal–organic chemical vapor deposition. The InGaN/GaN QW active region consisted of two periods of a 2.5-nm $In_{0.18}Ga_{0.82}N$ QW and a 6-nm GaN barrier. Moreover, a 20-nm $Al_{0.2}Ga_{0.8}N$ electron blocking layer was inserted on the top of the InGaN QWs to prevent carrier overflow.

The fabrication process of the device was similar to that reported in [20]–[22]. The device was fabricated using substrate transfer technique and laser lift-off process. Fig. 1 shows the schematic of the VCSEL and a surface photograph of a device. The current injecting aperture was formed using patterned SiO_2, and a 30-nm-thick indium tin oxide (ITO) layer was used as a current spreading layer. A 13.5-pair Ti_3O_5/SiO_2 bottom distributed Bragg reflectors (DBR) and an 11-pair Ti_3O_5/SiO_2 top DBR were used as cavity mirrors. Cr/Au was used for both p- and n-type electrodes.

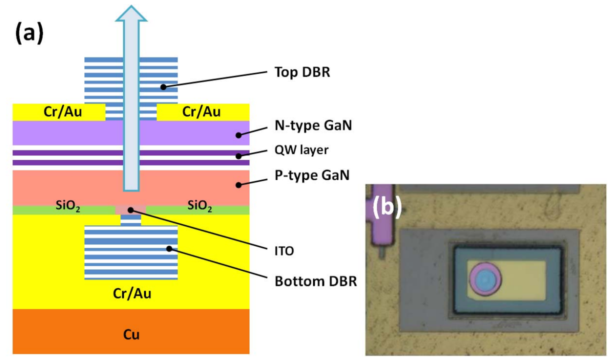

Fig. 1. (a) Cross-sectional schematic of the VCSEL. (b) Optical image of a real device.

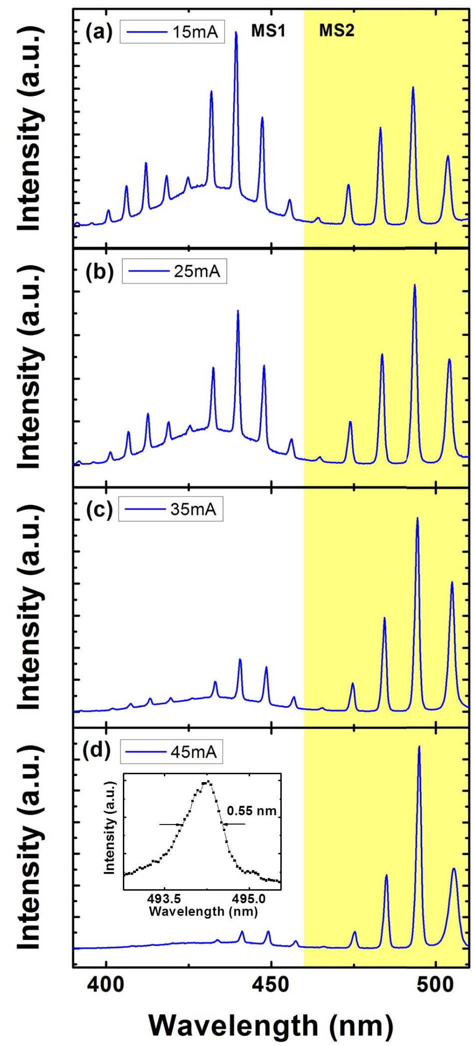

Fig. 2. EL spectra of the VCSEL measured at four different currents. (a) 15, (b) 25, (c) 35, and (d) 45 mA. Inset: linewidth of the laising peak measured with a higher resolution.

III. Results and Discussion

Fig. 2 presents the room temperature (RT) electroluminescence (EL) spectra measured from a device under different injection currents. The cavity effect is obvious that the gain of the active region is “channeled” into the cavity modes and the ON-resonance wavelengths are strongly enhanced. We divided the cavity modes into two groups: the cavity modes centered at the emission peak were defined as MS1, while the cavity modes centered at the emission edge were defined as MS2 (highlighted by the yellow-shaded area). Due to the cavity effect, carriers are captured mainly by the ON-resonance wavelengths because of the shorter lifetime of related recombination. For the cavity mode at MS1/MS2 boundary, the EL intensity is weak because of the less-gain enhancement factor or overlap between active region and the standing wave [32]. Under a current of 15 mA, the main mode in MS1 (440-nm mode) is stronger than the main mode in MS2 (493-nm mode). When the current is increased to 25 mA, the intensities of the main mode in MS1 and MS2 are almost equal. When the current reaches 35 mA, the change from SE to lasing is achieved and the emission color of the device changes from blue to green. The linewidth of the lasing peak is about 0.55 nm, as shown in the inset of Fig. 2(d). As the current is increased further, the lasing modes become dominant while MS1 and the background emission are suppressed.

For MS1, it originates from 2-D QWs. On the other hand, MS2 originates from InN-rich low-bandgap localization centers caused by the condensation of indium in the InGaN/GaN

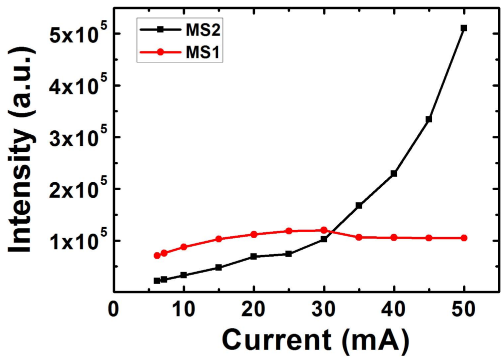

Fig. 3. Integrated EL intensity of MS1 and MS2 as a function of the injected current.

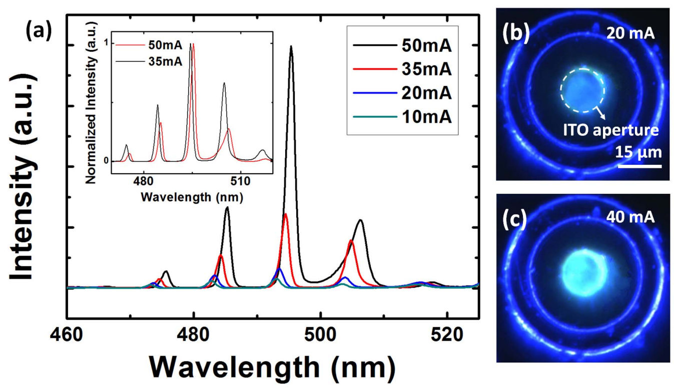

Fig. 4. (a) Enlarged EL spectra of the lasing region for different currents. Inset: normalized intensity of EL spectra at two different injection currents above threshold. Mode competition and peak shift were observed. Near-field patterns for device at (b) 20 and (c) 40 mA. The images were taken under low-gain settings to avoid saturating the camera. In the photographs, the luminous circles from inside to outside are ITO aperture, the interior boundary of n-type electrode, and the top DBR edge, respectively.

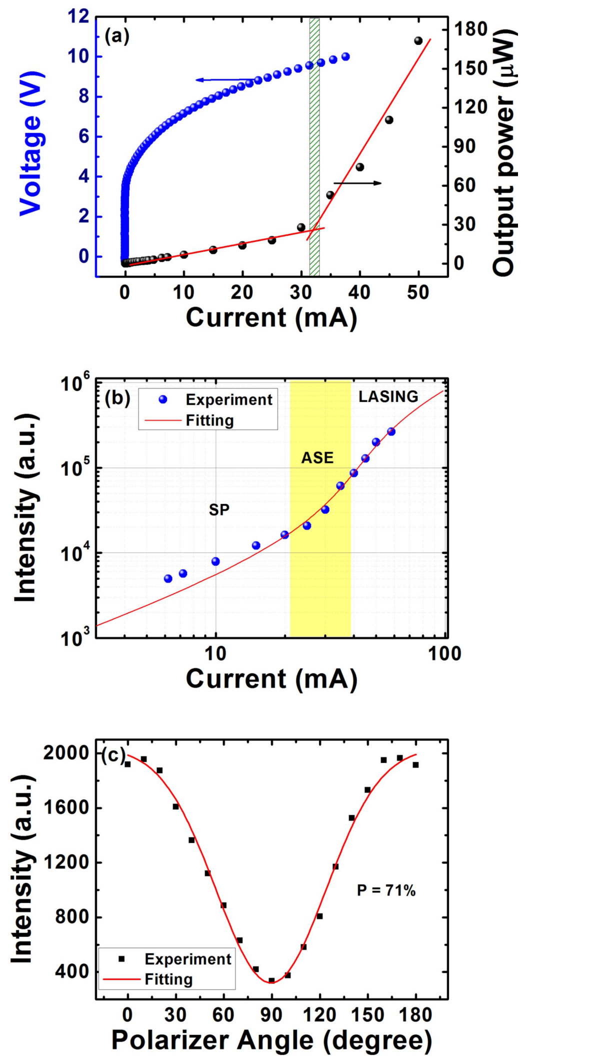

Fig. 5. (a) I–L and I–V characteristics of the VCSEL with a 15-μm-diameter current aperture under CW operation at 300 K. (b) Laser emission intensity versus injection current in logarithmic scale. The solid red curve represents a fit to the experimental data using a rate-equation model. (c) Polarization characteristics of the laser emission at an injection current of 1.09 I_{th}.

QW, which are similar to zero-dimensional structures such as QDs or color centers [33]. Generally, the carriers in the QW can freely move in the well-plane and be easily captured by the localization centers. The evolution of the spectra in Fig. 2 reflects the carrier capture and recombination related with two emission bands at different injection currents. The integrated EL intensity of MS1 and MS2 as a function of the injection current is shown in Fig. 3. At relatively small currents, MS1 is stronger than MS2. This can be understood when considering the low density of localized centers. With increasing current, much more carriers can be captured and recombine through the localization centers. In other words, MS2 exhibits a much faster growth rate and becomes stronger than MS1 with increasing current injection. At even larger currents, lasing can be achieved. Such phenomenon is attributed to the cavity-enhanced recombination, which will be discussed in the latter part of this paper.

Fig. 4(a) shows the evolution of the emission spectra of the lasing modes at different driving currents. It is clearly revealed that the intensity of the lasing peak increased dramatically above the threshold current. The relative intensity of different cavity modes was found to vary with increasing currents, as shown in the inset of Fig. 4(a). Above threshold, the main mode at ~493 nm is always dominant while the suppression of side modes becomes pronounced at the higher current. Compared with common microcavity light emitting diodes, this phenomenon of mode competition is a typical characteristic for lasers [34]. Near-field patterns of the device at 20 and 40 mA are shown in Fig. 4(b) and (c). The green light emitted from current aperture, and with a cavity, is strongly enhanced when the threshold condition is reached. On the other hand, the leakage light from the circular DBR edge, which is due to SE without the cavity effect, is always blue. This phenomenon demonstrates unambiguously that the green emission originates from the cavity effect.

Fig. 5(a) shows the current–light output (I–L) and current–voltage (I–V) characteristics of the device under RT continuous wave (CW) operation. To extract the threshold current, we applied linear fits to the I–L data below and above

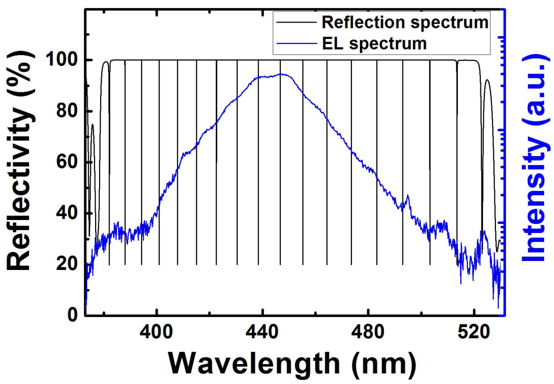

Fig. 6. Calculated reflection spectrum of the microcavity and measured EL spectrum of the device without top DBR. EL spectrum was plotted using a logarithmic scale on the *y*-axis.

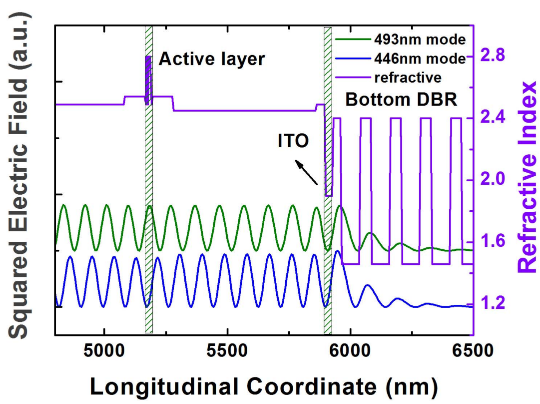

Fig. 7. Refractive index and the distribution of the optical field for the 446- and 493-nm cavity modes of the VCSEL.

the threshold. A threshold (I_{th}) was clearly observed around a current of 32 mA, and the threshold current density was found to be ~18 kA/cm^2. The output power of the device at 50 mA was ~178 μW. A rate-equation model is adopted to fit the experimental data of emission intensity versus current in logarithmic coordinates [35]. The "S" shape of L–I curve in logarithmic coordinate shows a standard lasing evolution process including SE region, amplified SE (ASE) region, and lasing region. The ASE regime is highlighted by the yellow-shaded area. Fig. 5(c) depicts the polarization characteristics of the VCSEL. Polarization measurements show that the degree of polarization is 71% under CW operation of 1.09 I_{th}, which is another evidence of lasing action. In addition, we fabricated the devices with different current aperture sizes. Since the lasing can be achieved at the same current density, the devices with smaller aperture size have lower junction temperature because of the lower current. This suggests that smaller devices have a better spectral stability.

Fig. 6 shows the simulation result of reflection spectrum and the measured EL spectrum of the device without top DBR, which equals approximately the gain band. Moreover, the emission spectrum is modulated by the cavity formed between bottom DBR and the top GaN/air interface. The DBR shows a wide stopband of about 140 nm. In our experiment, several cavity modes satisfying the gain-cavity alignment were observed, as shown in Fig. 2.

The lasing action benefits from the cavity-enhanced recombination. The recombination of excitons localized at certain potential minima is similar to "QDs" or some "color centers." However, due to the low density of such localization centers, the green emission intensity is low when there is no cavity, as can be seen from Fig. 6. When a cavity is applied, however, cavity effect causes significant enhancement in the recombination efficiency at resonant modes. For InGaN/GaN QWs, emission lifetimes of 155, ~100, and <25 ps (the system limit) for wafer only, half-cavity, and full-cavity structures, respectively, have been observed previously [31]. For a color center like silicon-vacancy in diamond, tenfold lifetime reduction and 42-fold enhancement in emission intensity were observed [29]. Therefore, the emission lifetime of the deep localized luminescence centers is expected to be significantly shortened when the emission coincides with the cavity mode. The short lifetime indicates a high carrier capture efficiency and can compensate the low density of emission centers, resulting in stronger emission intensity.

Another important factor is gain enhancement factor (Γr) which reflects the spatial overlap or coupling between the cavity mode and the emitting center and has a crucial effect on the lasing characteristics. Fig. 7 shows the optical field (squared electric field) of the 446- and 493-nm cavity modes calculated by the transfer matrix method. In calculation, the refractive indexes of Ti_3O_5 and SiO_2 are 2.4 and 1.465, and the thicknesses of Ti_3O_5 and SiO_2 are 46 and 75 nm, respectively. It can be seen that a good coupling between the active region and the antinode of the optical field for the 493-nm cavity mode is achieved. A better overlap means a larger gain enhancement factor, which can effectively decrease the threshold gain of the VCSEL [36]. Compared with the mode at 493 nm, however, the active region is overlapped more closely with the node of the standing wave for the 446-nm mode, resulting in a small gain enhancement factor. Γ_r is estimated to be 1.82 for 493 nm and 0.21 for 446 nm. The threshold current density is strongly dependent on Γ_r and increases exponentially with Γ_r reduction when Γ_r is smaller than 1 [32]. That is the reason why the 446-nm mode did not achieve lasing although this wavelength is near the peak of the EL emission band. Moreover, the longer lasing wavelength also benefits less absorption loss in the active region [16]. All these factors contribute to the lasing at 493 nm.

IV. Conclusion

In summary, we have demonstrated green GaN-based VCSELs using a normally blue-emitting QWs with a microcavity. The green light appears at the emission edge of the QW and comes from InN-rich lower bandgap. With a cavity, the cavity-mode matched localization centers are featured with enhanced emission efficiency. Combining with higher capture efficiency to injected carriers, the emission intensity shows superlinear increase with injection current, and eventually, lasing action is achieved. A threshold current of 32 mA (threshold current density ~18 kA/cm^2) and output power of 178 μW at 50 mA were observed. Our result presents novel opportunities for the design and fabrication of green VCSELs.

References

[1] Y. Hirano *et al.*, "Solid-state SHG green laser for laser TV," in *Proc. CLEO/QELS*, Baltimore, MD, USA, Jun. 2009, pp. 1–2, doi: 10.1364/iqec.2009.ptha3.

[2] H. K. Nguyen *et al.*, "304 mW green light emission by frequency doubling of a high-power 1060-nm DBR semiconductor laser diode," *Proc. SPIE*, vol. 6890, p. 68900I, Feb. 2008, doi: 10.1117/12.770678.

[3] S. Mokkapati and C. Jagadish, "III-V compound SC for optoelectronic devices," *Mater. Today*, vol. 12, no. 4, pp. 22–32, Apr. 2009, doi: 10.1016/S1369-7021(09)70110-5.

[4] H. Ohta, S. P. Denbaars, and S. Nakamura, "Future of group-III nitride semiconductor green laser diodes," *J. Opt. Soc. Amer. B, Opt. Phys.*, vol. 27, no. 11, pp. B45–B49, 2010, doi: 10.1364/JOSAB.27.000B45.

[5] S. Nakamura *et al.*, "InGaN-based multi-quantum-well-structure laser diodes," *J. Appl. Phys.*, vol. 35, no. 1B, pp. B45–B49, 1996, doi: 10.1143/JJAP.35.L74.

[6] F. A. Ponce and D. P. Bour, "Nitride-based semiconductors for blue and green light-emitting devices," *Nature*, vol. 386, no. 6623, pp. 351–359, Mar. 1997, doi: 10.1038/386351a0.

[7] S. Lutgen *et al.*, "True green InGaN laser diodes," *Phys. Status Solidi A*, vol. 207, no. 6, pp. 1318–1322, Jun. 2010, doi: 10.1002/pssa.200983620.

[8] X. H. Wu *et al.*, "Dislocation generation in GaN heteroepitaxy," *J. Cryst. Growth*, vols. 189–190, pp. 231–243, Jun. 1998, doi: 10.1016/S0022-0248(98)00240-1.

[9] T. Takeuchi *et al.*, "Quantum-confined Stark effect due to piezoelectric fields in GaInN strained quantum wells," *Jpn. J. Appl. Phys.*, vol. 36, no. 4A, pp. L382–L385, Apr. 1997, doi: 10.1143/jjap.36.l382.

[10] S. Fujita, "Wide-bandgap semiconductor materials: For their full Bloom," *Jpn. J. Appl. Phys.*, vol. 54, no. 3, p. 030101, Feb. 2015, doi: 10.7567/jjap.54.030101.

[11] D. F. Feezell, "Status and future of GaN-based vertical-cavity surface-emitting lasers," *Proc. SPIE*, vol. 9363, p. 93631G, Mar. 2015, doi: 10.1117/12.2079503.

[12] T.-C. Lu, C.-C. Kao, H.-C. Kuo, G.-S. Huang, and S.-C. Wang, "CW lasing of current injection blue GaN-based vertical cavity surface emitting laser," *Appl. Phys. Lett.*, vol. 92, no. 14, p. 141102, Apr. 2008, doi: 10.1063/1.2908034.

[13] T. C. Lu *et al.*, "Continuous wave operation of current injected GaN vertical cavity surface emitting lasers at room temperature," *Appl. Phys. Lett.*, vol. 97, no. 7, p. 071114, Aug. 2010, doi: 10.1063/1.3483133.

[14] G. Cosendey, A. Castiglia, G. Rossbach, J.-F. Carlin, and N. Grandjean, "Blue monolithic AlInN-based vertical cavity surface emitting laser diode on free-standing GaN substrate," *Appl. Phys. Lett.*, vol. 101, no. 15, p. 151113, Oct. 2012, doi: 10.1063/1.4757873.

[15] C. Holder, J. S. Speck, S. P. DenBaars, S. Nakamura, and D. Feezell, "Demonstration of nonpolar GaN-based vertical-cavity surface-emitting lasers," *Appl. Phys. Express*, vol. 5, no. 9, p. 092104, 2012, doi: 10.1143/APEX.5.092104.

[16] C. A. Forman *et al.*, "Continuous-wave operation of m-plane GaN-based vertical-cavity surface-emitting lasers with a tunnel junction intracavity contact," *Appl. Phys. Lett.*, vol. 112, no. 11, p. 111106, Mar. 2018, doi: 10.1063/1.5007746.

[17] T. Furuta *et al.*, "Room-temperature CW operation of a nitride-based vertical-cavity surface-emitting laser using thick GaInN quantum wells," *Jpn. J. Appl. Phys.*, vol. 55, no. 5S, p. 05FJ11, Apr. 2016, doi: 10.7567/JJAP.55.05FJ11.

[18] K. Ikeyama *et al.*, "Room-temperature continuous-wave operation of GaN-based vertical-cavity surface-emitting lasers with n-type conducting AlInN/GaN distributed Bragg reflectors," *Appl. Phys. Express*, vol. 9, no. 10, p. 102101, Sep. 2016, doi: 10.7567/APEX.9.102101.

[19] P. S. Yeh *et al.*, "GaN-based vertical-cavity surface emitting lasers with sub-milliamp threshold and small divergence angle," *Appl. Phys. Lett.*, vol. 109, no. 24, p. 241103, Dec. 2016, doi: 10.1063/1.4972182.

[20] G. Weng *et al.*, "Low threshold continuous-wave lasing of yellow-green InGaN-QD vertical-cavity surface-emitting lasers," *Opt. Express*, vol. 24, no. 14, pp. 15546–15553, Jul. 2017, doi: 10.1364/oe.24.015546.

[21] Y. Mei *et al.*, "Quantum dot vertical-cavity surface-emitting lasers covering the 'green gap,'" *Light, Sci. Appl.*, vol. 6, no. 1, p. e16199, Jan. 2017, doi: 10.1038/lsa.2016.199.

[22] R. B. Xu *et al.*, "Simultaneous blue and green lasing of GaN-based vertical-cavity surface-emitting lasers," *Semicond. Sci. Technol.*, vol. 32, no. 10, p. 105012, Sep. 2017, doi: 10.1088/1361-6641/aa87aa.

[23] Y. Higuchi, K. Omae, H. Matsumura, and T. Mukai, "Room-temperature CW lasing of a GaN-based vertical-cavity surface-emitting laser by current injection," *Appl. Phys. Express*, vol. 1, no. 12, p. 121102, Dec. 2008, doi: 10.1143/APEX.1.121102.

[24] K. Omae, Y. Higuchi, K. Nakagawa, H. Matsumura, and T. Mukai, "Improvement in lasing characteristics of GaN-based vertical-cavity surface-emitting lasers fabricated using a GaN substrate," *Appl. Phys. Express*, vol. 2, no. 5, p. 052101, Apr. 2009, doi: 10.1143/APEX.2.052101.

[25] D. Kasahara *et al.*, "Demonstration of blue and green GaN-based vertical-cavity surface-emitting lasers by current injection at room temperature," *Appl. Phys. Express*, vol. 4, no. 7, p. 072103, Jun. 2011, doi: 10.1143/apex.4.072103.

[26] T. Onishi, O. Imafuji, K. Nagamatsu, M. Kawaguchi, K. Yamanaka, and S. Takigawa, "Continuous wave operation of GaN vertical cavity surface emitting lasers at room temperature," *IEEE J. Quantum Electron.*, vol. 48, no. 9, pp. 1107–1112, Sep. 2012, doi: 10.1109/JQE.2012.2203586.

[27] S. Izumi, N. Fuutagawa, T. Hamaguchi, M. Murayama, M. Kuramoto, and H. Narui, "Room-temperature continuous-wave operation of GaN-based vertical-cavity surface-emitting lasers fabricated using epitaxial lateral overgrowth," *Appl. Phys. Express*, vol. 8, no. 6, p. 062702, May 2015, doi: 10.7567/APEX.8.062702.

[28] T. Hamaguchi, N. Fuutagawa, S. Izumi, M. Murayama, and H. Narui, "Milliwatt-class GaN-based blue vertical-cavity surface-emitting lasers fabricated by epitaxial lateral overgrowth," *Phys. Status Solidi A*, vol. 213, no. 5, pp. 1170–1176, Jan. 2016, doi: 10.1002/pssa.201532759.

[29] J. L. Zhang *et al.*, "Strongly cavity-enhanced spontaneous emission from silicon-vacancy centers in diamond," *Nano Lett.*, vol. 18, no. 2, pp. 1360–1365, Jan. 2018, doi: 10.1021/acs.nanolett.7b05075.

[30] H. Yokoyama, K. Nishi, T. Anan, H. Yamada, S. D. Brorson, and E. P. Ippen, "Enhanced spontaneous emission from GaAs quantum wells in monolithic microcavities," *Appl. Phys. Lett.*, vol. 57, no. 26, pp. 2814–2816, 1990, doi: 10.1063/1.103771.

[31] Y. T. He *et al.*, "The characteristics of optical pumped GaN-based vertical cavity surface emitting laser structures," *Appl. Mech. Mater.*, vol. 692, pp. 187–190, Nov. 2014, doi: 10.1109/leos.1993.379314.

[32] Y. Mei *et al.*, "Tunable InGaN quantum dot microcavity light emitters with 129 nm tuning range from yellow-green to violet," *Appl. Phys. Lett.*, vol. 111, no. 12, p. 121107, Sep. 2017, doi: 10.1063/1.4994945.

[33] S. F. Chichibu *et al.*, "Origin of defect-insensitive emission probability in In-containing (Al,In,Ga)N alloy semiconductors," *Nature Mater.*, vol. 5, pp. 810–816, Sep. 2006, doi: 10.1038/nmat1726.

[34] M. Ahmed and M. Yamada, "Influence of instantaneous mode competition on the dynamics of semiconductor lasers," *IEEE J. Quantum Electron.*, vol. 38, no. 6, pp. 682–693, Jun. 2002, doi: 10.1109/JQE.2002.1005419.

[35] G. Bjork and Y. Yamamoto, "Analysis of semiconductor microcavity lasers using rate equations," *IEEE J. Quantum Electron.*, vol. 27, no. 11, pp. 2386–2396, Nov. 1991, doi: 10.1109/3.100877.

[36] R. Michalzik, *Fundamentals, Technology and Applications of Vertical-Cavity Surface-Emitting Lasers*. Berlin, Germany: Springer, 2013, pp. 27–30.

Rongbin Xu received the B.S. degree in microelectronics from Fuzhou University, Fuzhou, China, in 2015. He is currently pursuing the Ph.D. degree with the Department of Electronic Engineering, Xiamen University, Xiamen, China.

His current research interests include the III-nitride semiconductor device fabrication and characterization, especially GaN-based vertical-cavity surface-emitting lasers.

Yang Mei received the bachelor's degree in electronic and information engineering from the China University of Geosciences, Wuhan, China, in 2014. He is currently pursuing the Ph.D. degree with the Department of Electronic Engineering, Xiamen University, Xiamen, China.

His current research interests include GaN-based quantum dots and vertical-cavity surface-emitting lasers.

Huan Xu received the B.S. degree from the School of Information Science and Engineering, Xiamen University, Xiamen, China, in 2017, where she is currently pursuing the master's degree with the College of Microelectronics and Solid State Electronics.

Her current research interests include vertical-cavity surface-emitting lasers.

Lei-Ying Ying was born in Guangzhou, China, in 1963. She received the B.S. degree in physics from Zhongshan University, Guangzhou, in 1983, and the M.E. degree in electronic engineering from the Hebei Semiconductor Research Institute, Shijiazhuang, China, in 1986.

In 2011, she joined the Department of Physics, Xiamen University, Xiamen, China. Her current research interests include microfabrication/nanofabrication and semiconductor devices for optoelectronic applications.

Zhiwei Zheng received the B.E. degree from the Nanjing University of Science and Technology, Nanjing, China, in 2008, and the Ph.D. degree from the Institute of Microelectronics of Chinese Academy of Sciences, Beijing, China, in 2014.

He is currently an Assistant Professor with Xiamen University, Xiamen, China. His current research interests include nanofabrication and semiconductor devices for optoelectronic applications.

Hao Long was born in Ji'an, JiangXi, China, in 1986. He received the B.S. and Ph.D. degrees in physics from Peking University, Beijing, China, in 2008 and 2013, respectively.

From 2013 to 2015, he was a Staff Researcher with Lenovo Inc., Beijing. In 2015, he joined the Department of Electrical Engineering, Xiamen University, Xiamen, China, as a Post-Doctoral Researcher, where he has been an Assistant Professor since 2017.

Dan Zhang received the Ph.D. degree from Jilin University, Changchun, China, in 2008.

She joined the Department of Electronic Engineering, Xiamen University, Xiamen, China. Her current research interests include optical sensors.

Baoping Zhang was born in Shijiazhuang, Hebei, China, in 1963. He received the B.S. degree in physics from Lanzhou University, Lanzhou, China, in 1983, the M.E. degree in electronic engineering from the Hebei Semiconductor Research Institute, Shijiazhuang, China, in 1986, and the Dr.-Eng. degree in applied physics from the University of Tokyo, Tokyo, Japan, in 1994.

He is currently a Distinguished Professor with the College of Electronic Science and Technology.

Jianping Liu received the Ph.D. degree in microelectronics and solid-state electronics from the Institute of Semiconductors, Chinese Academy of Sciences, Beijing, China, in 2004.

From 2006 to 2010, he was a Post-Doctoral Researcher with the Georgia Institute of Electronics and Computer Engineering, Atlanta, GA, USA. He is currently a Professor with the Suzhou Institute of Nano-Tech and Nano-Bionics, Chinese Academy of Sciences, Suzhou, China.